Program Digest, 2019 IEEE International Ultrasonics Symposium (IUS)
Glasgow, Scotland, October 6-9, 2019

Towards flow Estimation in the Common Carotid Artery Using Free-Hand Cross-Sectional Doppler

Luuk van Knippenberg*, Ruud JG van Sloun*, Sergei Shulepov†, Arthur Bouwman‡ and Massimo Mischi*
*Lab. of Biomedical Diagnostics, Eindhoven University of Technology, the Netherlands
†Multiphysics and Optics, Philips Research Eindhoven, the Netherlands
‡Anesthesiology and Pain Medicine, Catharina Hospital Eindhoven, the Netherlands
Email: l.a.e.m.v.knippenberg@tue.nl

***Abstract*—Quantifying blood flow is of major clinical importance for the assessment of the cardiovascular status. Longitudinal flow measurements in the common carotid suffer from operator-dependency and are very sensitive to motion. In this work, a method is proposed to perform flow estimation from cross-sectional acquisitions, which reduces operator-dependency and is more robust to motion. By modeling the vessel as a cylinder, the intersection between the ultrasound plane and the vessel is an ellipse. The properties of this ellipse (semi-major and semi-minor axis, rotation and center position) are used to estimate the Doppler angle (beam-to-flow angle). This method was tested *in vitro* on a constant flow phantom using a wide variety of Doppler angles, where the errors in the flow estimates were below 10%. Further research should aim at quantifying the sensitivity of this method and validating this method *in vivo*.**

I. Introduction

Cardiac output is the amount of blood that is pumped by the left ventricle through the aorta in one minute. It is often monitored during surgery to assess the cardiac function and condition [1] [2]. However, a method that is accurate, precise, operator-independent, dynamic, continuous, non-invasive and easy to use does not exist today [3]. The current gold standard, thermodilution, is highly invasive because of the need for central catheterization and may cause serious complications, whereas the most popular non-invasive method, Doppler echocardiography, suffers from a large inter-operator variability and requires an experienced operator [4]. Rather than measuring cardiac output, it might be valuable to measure blood flow in major arteries, which are still close to the heart but are more accessible for ultrasound, such as the common carotid artery (CCA). In this case, flow trends and variations can monitored non-invasively.

To estimate flow, both cross-sectional area and blood velocity have to be measured. In clinical practice, this is achieved by imaging the vessel longitudinally, where the probe is positioned parallel to the vessel. Assuming that the vessel has a circular cross-section, the cross-sectional area can be determined from the diameter of the vessel. This diameter measurement strongly depends on the skills of the operator as the center of the vessel has to be well aligned with the transducer, otherwise the diameter will be underestimated. Blood velocity can be determined through the Doppler equation:

$$v = \frac{cf_d}{2\cos(\alpha)f_0}, \tag{1}$$

where c is the speed of sound in tissue, f_d is the Doppler frequency shift, α is the Doppler angle (angle between the insonifying beam and blood flow direction) and f_0 is the transmit frequency. If the flow is assumed to be laminar (parallel to the vessel wall), the Doppler angle can be determined directly from the B-mode image since the direction of both, the beam and flow vector, is known. However, the flow direction has to be set manually, which introduces room for errors in the angle correction. In addition to this large operator-dependency, the longitudinal flow measurement has the disadvantage that it is sensitive to motion; if either the patient or the transducer moves, the transducer has to be repositioned. Due to the difficulty in acquiring and maintaining a perfect longitudinal image, this method is not suitable for long-term monitoring of flow.

In contrast, the measurement is more robust to motion when imaging the vessel cross-sectionally, similar to the methods proposed by Kitabatake *et al.* [5], Picot *et al.* [6] and Schorer *et al.* in [7]. In this case, the cylindrical vessel appears as an ellipse on the B-mode image and a smaller, yet unknown, Doppler angle can be realized by tilting the transducer. The above works leverage that, for a vertical ellipse, the Doppler angle can be derived from the semi-major axis, a, and semi-minor axis, b, of the ellipse. However, maintaining a vertical ellipse requires precise positioning of the transducer with respect to the vessel, thereby still suffering from operator-dependency.

In this work, a method is proposed in which flow is estimated from fully free-hand cross-sectional ultrasound acquisitions, being more flexible in placement. This reduces operator-dependency and makes long-term flow monitoring more feasible. Using a geometrical model consisting of the intersection between a plane and cylinder, it is shown in Section II that the Doppler angle can be estimated from the parameters of the resulting ellipse such as its semi-major axis, semi-minor axis, orientation and center by solving a least-squares problem, which is then leveraged to correct the measured velocities. The performance of this method is assessed by *in-vitro* measurements, of which the method is described in Section III and the results are reported in Section IV. Finally, in Section V the results are discussed and conclusions are derived.

II. Methods

A. Doppler angle estimation

Under the assumption that the vessel can be modeled as a cylinder and the ultrasound plane as a two dimensional plane, the intersection of the vessel and plane can be modeled as an ellipse. By finding an analytical expression for this ellipse as it appears on the B-mode image, the Doppler angle can be estimated from the ellipse parameters. This analytical expression is derived in this Section.

We start from a right-handed coordinate system where the center of the transducer is defined as the origin, the vessel (cylinder) is parallel to the x-axis and the z-axis represents depth. The initial orientation of the transducer is along the y-axis such that the ultrasound plane is spanned by the vectors $\vec{u_1} = [0, 1, 0]^T$ and $\vec{u_2} = [0, 0, -1]^T$. Next, the transducer is first rotated by θ around the z-axis followed by a rotation of φ around the new (rotated) y-axis. This situation is illustrated in Fig. 1(a) where the plane is rotated by $\theta = 20°$ and $\varphi = -30°$ and the vessel radius is 5 mm. By using rotational matrices we find that the spanning vectors of the rotated plane are $\vec{u_{1r}} = [-\sin(\theta), \cos(\theta), 0]^T$ and $\vec{u_{2r}} = [-\cos(\theta)\sin(\varphi), -\sin(\theta)\sin(\varphi), -\cos(\varphi)]^T$. The normal vector of the plane, n, is then defined as the cross product of these spanning vectors:

$$\vec{n} = \begin{bmatrix} x_n \\ y_n \\ z_n \end{bmatrix} = \vec{u_{1r}} \times \vec{u_{2r}} = \begin{bmatrix} -\cos(\theta)\cos(\varphi) \\ -\sin(\theta)\cos(\varphi) \\ \sin(\varphi) \end{bmatrix}. \quad (2)$$

Given that the plane moves through the origin of the chosen coordinate system, the plane equation can be written as:

$$-\cos(\theta)\cos(\varphi)x - \sin(\theta)\cos(\varphi)y + \sin(\varphi)z = 0. \quad (3)$$

Next, if a parametric representation of the cylinder with radius R along the x-axis is used:

$$\begin{cases} y(t) = R \cdot \cos(t) + y_0 \\ z(t) = R \cdot \sin(t) + z_0 \end{cases}, \quad (4)$$

the x-coordinate of the 3D intersection can be written as:

$$x_i(t) = -\tan(\theta)y(t) + \frac{\tan(\varphi)}{\cos(\theta)}z(t). \quad (5)$$

Lastly, the initial rotation that was used to obtain the rotated spanning vectors is reversed such that these 3D coordinates are in the B-mode (yz)-plane:

$$f(t, \mathbf{w}) = \begin{cases} y_p = & \frac{1}{\cos(\theta)}y(t) - \tan(\theta)\tan(\varphi)z(t) \\ z_p = & \frac{1}{\cos(\varphi)}z(t) \end{cases}, \quad (6)$$

where $\mathbf{w} = [\theta, \varphi, R, x_0, z_0]^T$. The shape of the ellipse in the resulting B-mode image thus depends on the rotation of the transducer with respect to the vessel and the radius and location of the vessel.

We estimate the ellipse shape from the ultrasound B-mode image through a dedicated vessel segmentation strategy, resulting in N points on the vessel wall. We detail on this in section IIB. From these N points, we obtain the parameters $\mathbf{w}$ through a least-squares approach using the trust-region-reflective algorithm of MATLAB (Mathworks, MA, USA). The Doppler angle is then estimated as the angle between the beam vector (equal to $\vec{u_{2r}}$ if no beamsteering is used) and the flow vector (parallel to the x-axis):

$$\hat{\alpha} = \arccos(-\cos(\theta)\sin(\varphi)). \quad (7)$$

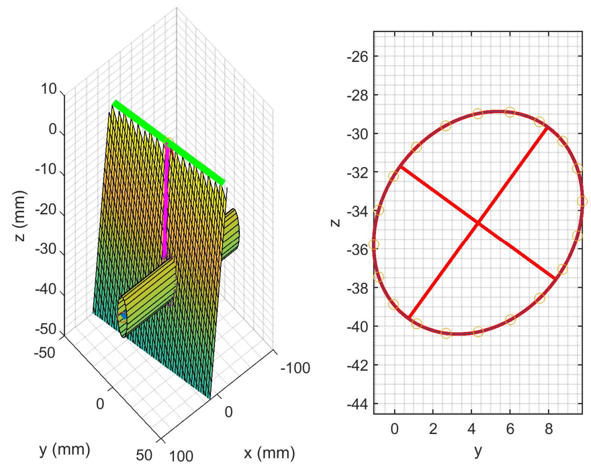

(a) (b)

Fig. 1. (a): 3D visualization of a tilted and rotated plane ($\theta = 20°$ and $\varphi = -30°$) intersecting with a cylindrical vessel ($R = 5$ mm). (b): Elliptical intersection of the plane and cylinder with semi-major axis 6.14 mm, semi-minor axis 5.00 mm, and the ellipse is rotated 53.95° with respect to the x-axis.

B. Vessel segmentation

Many classical image segmentation algorithms are gradient-based, with local maxima in such gradient maps representing transitions. Due to speckle and noise, the intensity gradient that is measured in a B-mode image of a vessel however typically contains multiple peaks rather than only the peaks that correspond to the transitions between tissue and vessel [8]. Therefore, a more sophisticated approach is used to segment the vessel from cross-sectional ultrasound images. First, a seed point is manually positioned, which ideally corresponds to the center of the vessel. From this point, 128 radial lines are drawn on the B-mode image, similarly to the spokes ellipse algorithm given in [9]. Next, a set of Gaussian smoothed images is generated and for each spoke the edge is detected in the most smoothed image. This edge is then tracked through a series of progressively less smoothed images by selecting the peak in image gradient that is closest to the previously-found peak until the edge in the original, noisy image is detected for each of the spokes. This results in 128 points on the vessel wall. Outliers are detected and removed by using a moving median filter (length 10 points). Finally, an ellipse was fitted to all the remaining points.

III. Experimental methods

A. Measurement setup

Measurements were performed on a custom flow phantom, which consists of a straight tube (6 mm inner diameter, 1 mm wall thickness) placed inside tissue mimicking material at a depth of 20 mm from the imaging surfaces. Both the tube (vessel) and its surroundings (tissue) are made using a synthetic polymer PolyVinyl Alcohol (PVA) solution, with the only difference being the concentration of Silica gel particles (ultrasound scatterers). The procedure described in [10] was followed to obtain the PVA solution. The phantom was connected to a Liquiflo flow pump model H3F (Liquiflo Equipment Company, Garwood, NJ, USA), controlled using Labview (National Instruments, Austin, TX, USA). The pump circulated blood-mimicking fluid (Shelley Medical Imaging Technologies, London, ON, CA) at a constant flow rate of 334 mL/min (verified with a flow sensor) such that Doppler measurements can be performed. A commercial ultrasound scanner, Philips (Philips Healthcare, Bothell, WA, USA) EPIQ 7G, was used with a linear transducer (L12-3) to acquire ultrasound data.

First, ten longitudinal three-second acquisitions were performed, serving as reference. After acquiring data in both duplex and B-mode imaging modes, the transducer was repositioned to assess intra-operator-dependency in placement.

Next, cross-sectional images were acquired from 18 different orientations. For each orientation, a B-mode image, color Doppler image and power Doppler image were acquired.

B. Data analysis

For the longitudinal acquisitions, data analysis consists of diameter estimation from the B-mode image and velocity estimation from the color Doppler image. First, the pixel intensities along a vertical line are evaluated to detect the vessel wall and estimate vessel diameter. Second, along this same vertical line, the velocity profile $u(r)$ is extracted by mapping pixel color to velocity using the velocity scale in the color Doppler image. The velocity profile is integrated and corrected for the steering angle to find the average velocity v_{avg}. Diameter and velocity are both estimated for each frame and averaged over the three seconds of data. As the flow is constant and hence time-independent, the flow (in mL/min) can be estimated using:

$$Q = 60\pi R^2 v_{avg}. \tag{8}$$

For the cross-sectional acquisitions, first the vessel is segmented as described in Section II-B, from which the vessel diameter is estimated (equal to the minor axis of the fitted ellipse). Next, the power Doppler image is binarized and an ellipse is fit to this binary image that has the same normalized second central moments as the region [11]. The Doppler angle is then estimated from the properties of this ellipse as explained in Section II-A. Three measurements were discarded because the Doppler angle was larger than 70°, which is not representative of clinical measurements. Finally, the velocity profile along the short-axis of the ellipse is estimated from the color Doppler image, and the flow is determined.

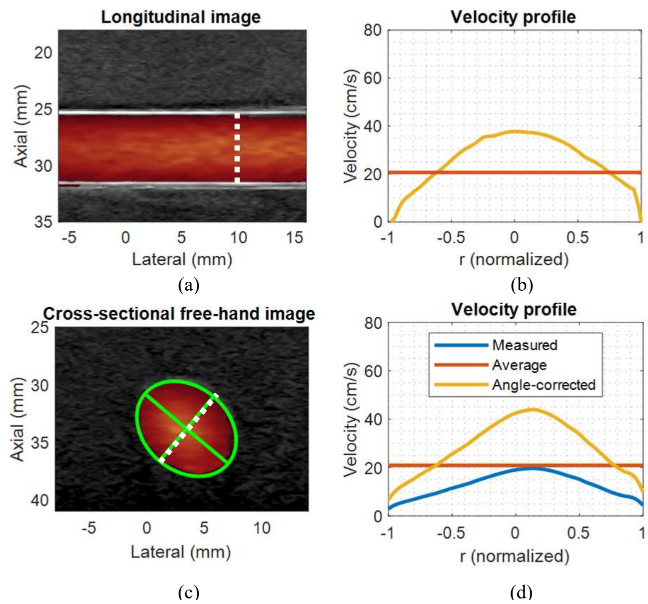

Fig. 2. Color Doppler image of longitudinal reference measurement (a) and the corresponding velocity profile and average velocity along the dashed line (b) compared to the cross-sectional free-hand measurement (c) and the velocity estimate (d). The Doppler angle in the cross-sectional measurement is estimated to be 63.4°. After correcting the measured velocity profile for this angle, the average estimated velocity corresponds well to the average velocity derived from the longitudinal acquisition (20.87 vs 20.62 cm/s).

IV. Results

Across the ten longitudinal measurements the diameter was estimated to be 5.69 ± 0.10 mm, the average velocity in the vessel 20.6 ± 0.5 cm/s and the flow 314.6 ± 12.1 mL/min. The best-aligned measurement having the largest diameter was used as reference. The corresponding flow estimate (333 mL/min) agrees well to the true flow rate (334 mL/min). Figure 2(a) shows the color Doppler image that corresponds to the this reference measurement, where the parabolic velocity profile along the dashed line is plotted in Fig. 2(b). From this velocity profile the average velocity is derived (20.62 cm/s), which together with the diameter estimate (5.85 mm) results in an accurate flow estimate.

An example of a cross-sectional free-hand color Doppler acquisition is shown in Fig. 2(c). The Doppler angle in this case is estimated to be 63.4°. The velocity profile along the short-axis of the ellipse is shown in Fig. 2(d) as the blue line, which after correcting for the Doppler angle corresponds well to the reference velocity profile and average velocity. Also, the estimated average velocity in the vessel shows good agreement with the longitudinal reference measurement.

The velocity before and after angle correction, Doppler angle, correction factor, diameter and flow are estimated for all 15 cross-sectional measurements. The results are summarized in Table I by the range, mean and standard deviation of each quantity. As a reference, the estimates from the longitudinal

TABLE I
ESTIMATED QUANTITIES FOR 15 CROSS-SECTIONAL FREE-HAND IN-VITRO MEASUREMENTS. TRUE FLOW WAS 334 ML/MIN AND UNLOADED DIAMETER WAS 5.9 MM. THE PARAMETERS ESTIMATED FROM A LONGITUDINAL ACQUISITION (AVERAGED OVER 3 SECONDS DATA) ARE USED AS REFERENCE.

Quantity	Min-Max	Mean $\pm$ std	Reference
Measured velocity (cm/s)	$7.90 - 10.54$	8.97 ± 0.67	NA
Doppler angle ($^\circ$)	$53.2 - 67.9$	63.7 ± 3.85	NA
Correction factor	$1.67 - 2.66$	2.29 ± 0.27	NA
Angle-corrected velocity (cm/s)	$17.45 - 22.44$	20.40 ± 1.52	20.62
Diameter (mm)	$5.68 - 6.16$	5.93 ± 0.13	5.85
Flow (mL/min)	$294 - 372$	337 ± 24	333

measurements are given in the right column. Over this wide range of Doppler angles, the estimated angle-corrected velocity shows good agreement to the reference velocity and the mean diameter estimate is accurate (5.93 mm vs 5.86 mm), resulting in flow estimates that are close to the true value (337 vs 334 mL/min).

V. DISCUSSION AND CONCLUSION

In this work, we presented a method to estimate blood flow in major arteries using cross-sectional Doppler acquisitions. In contrast to longitudinal acquisitions, cross-sectional Doppler is more robust to motion (probe motion or tissue motion), reducing the operator-dependency and allowing measurements over longer periods of time. The Doppler angle is estimated from the properties of the elliptical intersection (semi-major and semi-minor axis, rotation and position of center) between the cylindrical vessel and ultrasound plane. *In vitro* it was shown over a variety of Doppler angles that the flow can be estimated within 10% error, which is promising. This error is partly due to the the difficulty in segmenting the vessel from the B-mode image, which is evident from the large range in estimated diameter (0.5 mm difference between the minimal and maximal estimate). The difficulty arises from the fact that the ultrasound plane intersects the vessel under an angle, reducing the intensity of the received echo, resulting in blurred edges in the B-mode image.

To accurately determine the ellipse parameters required for the Doppler angle estimation, a power Doppler image was acquired in addition to the B-mode image (used for diameter estimation) and color Doppler image (used for velocity estimation). The power Doppler image is easy to binarize to regions where flow is present and where not, simplifying segmentation. Alternative segmentation methods, such as methods based on deep-learning [12] or snakes [13] [14], may improve the diameter estimate from the B-mode image, resulting in a more accurate flow estimate.

In addition to using an alternative segmentation method, future research should aim at evaluating the sensitivity of this method to errors in the estimated ellipse parameters. Factors that affect this sensitivity may include the resolution of the image, the Doppler angle and the circularity of the vessel. Finally, these results should be validated *in vivo* on a large population.

ACKNOWLEDGMENT

This study has been performed in the framework of the IMPULS2-program within the Eindhoven University of Technology in collaboration with Philips and the Catharina Hospital Eindhoven. The authors would like to thank John van Rooij (Philips Research Eindhoven) for his assistance on the phantom setup and Denny Mathews (Philips Research Eindhoven) for her suggestions and support during this research.

REFERENCES

[1] M. R. Pinsky, “Why measure cardiac output?” *Critical Care*, vol. 7, no. 2, pp. 114–116, 2003.
[2] J. Alhashemi, M. Cecconi, and C. Hofer, “Annual update in intensive care and emergency medicine,” in *Annual update in intensive care and emergency medicine*, J. Vincent, Ed. Springer, 2011, pp. 443–456.
[3] B. F. Geerts, L. P. Aarts, and J. R. Jansen, “Methods in pharmacology: Measurement of cardiac output,” *British Journal of Clinical Pharmacology*, vol. 71, no. 3, pp. 316–330, 2011.
[4] J. Y. Lefrant, P. Bruelle, A. G. Aya, G. Saïssi, M. Dauzat, J. E. De La Coussaye, and J. J. Eledjam, “Training is required to improve the reliability of esophageal Doppler to measure cardiac output in critically ill patients,” *Intensive Care Medicine*, vol. 24, no. 4, pp. 347–352, 1998.
[5] A. Kitabatake, J. Tanouchi, Y. Yoshida, T. Masuyama, M. Uematsu, and T. Kamada, “Quantitative color flow imaging to measure the two-dimensional distribution of blood flow velocity and the flow rate.” *Japanese circulation journal*, vol. 54, no. 3, pp. 304–308, mar 1990.
[6] P. A. Picot, M. Fruitman, R. N. Rankin, and A. Fenster, “Rapid volume flow rate estimation using transverse colour Doppler imaging,” *Ultrasound in Medicine and Biology*, vol. 21, no. 9, pp. 1199–1209, 1995.
[7] R. Schorer, A. Badoual, B. Bastide, A. Vandebrouck, M. Licker, and D. Sage, “A feasability study of color flow doppler vectorization for automated blood flow monitoring,” *Journal of Clinical Monitoring and Computing*, vol. 31, no. 6, pp. 1167–1175, 2017.
[8] F. Molinari, G. Zeng, and J. S. Suri, “A state of the art review on intima-media thickness (IMT) measurement and wall segmentation techniques for carotid ultrasound,” *Computer Methods and Programs in Biomedicine*, vol. 100, no. 3, pp. 201–221, 2010.
[9] D. Wang, R. Klatzky, B. W. B. Wu, G. Weller, a.R. Sampson, and G. Stetten, “Fully Automated Common Carotid Artery and Internal Jugular Vein Identification and Tracking Using B-Mode Ultrasound,” *IEEE Transactions on Biomedical Engineering*, vol. 56, no. 6, pp. 1691–1699, 2009.
[10] S. Fekkes, A. E. Saris, M. M. Nillesen, J. Menssen, H. H. Hansen, and C. L. De Korte, “Simultaneous vascular strain and blood vector velocity imaging using high-frequency versus conventional-frequency plane wave ultrasound: A phantom study,” *IEEE Transactions on Ultrasonics, Ferroelectrics, and Frequency Control*, vol. 65, no. 7, pp. 1166–1181, 2018.
[11] R. M. Haralick and L. G. Shapiro, *Computer and Robot Vision*, 1st ed. Boston, MA, USA: Addison-Wesley Longman Publishing Co., Inc., 1992.
[12] C. P. Loizou, “A review of ultrasound common carotid artery image and video segmentation techniques,” *Medical & Biological Engineering & Computing*, vol. 52, no. 12, pp. 1073–1093, 2014. [Online]. Available: http://link.springer.com/10.1007/s11517-014-1203-5
[13] R. Sanz-Requena, D. Moratal, D. R. García-Sánchez, V. Bodí, J. J. Rieta, and J. M. Sanchis, “Automatic segmentation and 3D reconstruction of intravascular ultrasound images for a fast preliminar evaluation of vessel pathologies,” *Computerized Medical Imaging and Graphics*, vol. 31, no. 2, pp. 71–80, 2007.
[14] D. Barbosa, T. Dietenbeck, J. Schaerer, J. D’hooge, D. Friboulet, and O. Bernard, “B-spline explicit active surfaces: An efficient framework for real-time 3-d region-based segmentation,” *IEEE Transactions on Image Processing*, vol. 21, no. 1, pp. 241–251, Jan 2012.